

## Measurements of Tau-Lepton Production and Decay

PLUTO Collaboration

Ch. Berger, H. Genzel, W. Lackas<sup>a</sup>, J. Pielorz<sup>b</sup>, F. Raupach, W. Wagner<sup>c</sup>

I. Physikalisches Institut der RWTH Aachen<sup>d</sup>, D-5100 Aachen, Federal Republic of Germany

A. Klovning, E. Lillestøl

University of Bergen<sup>e</sup>, N-5014 Bergen, Norway

J. Bürger, L. Criegee, A. Deuter, F. Ferrarotto<sup>f</sup>, G. Franke, M. Gaspero<sup>f</sup>,

Ch. Gerke<sup>g</sup>, G. Knies, B. Lewendel, J. Meyer, U. Michelsen, K.H. Pape,

B. Stella<sup>f</sup>, U. Timm, G.G. Winter, M. Zachara<sup>h</sup>, W. Zimmermann

Deutsches Elektronen-Synchrotron (DESY), D-2000 Hamburg, Federal Republic of Germany

P.J. Bussey, S.L. Cartwright<sup>i</sup>, J.B. Dainton, B.T. King<sup>j</sup>, C. Raine, J.M. Scarr,

I.O. Skillicorn, K.M. Smith, J.C. Thomson<sup>k</sup>

University of Glasgow<sup>l</sup>, Glasgow G128QX, UK

O. Achterberg<sup>m</sup>, V. Blobel, D. Burkart, K. Diehlmann, M. Feindt, H. Kapitza<sup>n</sup>,

B. Koppitz, M. Krüger<sup>o</sup>, M. Poppe, H. Spitzer, R. van Staa

II. Institut für Experimentalphysik der Universität, D-2000 Hamburg<sup>d</sup>, Federal Republic of Germany

C.Y. Chang, R.G. Glasser, R.G. Kellogg, S.J. Maxfield<sup>p</sup>, R.O. Polvado<sup>q</sup>,

B. Sechi-Zorn<sup>b</sup>, J.A. Skard, A. Skuja, A.J. Tylka, G.E. Welch, G.T. Zorn

University of Maryland<sup>r</sup>, College Park, MD 20742, USA

F. Almeida<sup>s</sup>, A. Bäcker, F. Barreiro, S. Brandt, K. Derikum<sup>t</sup>, C. Grupen,

H.J. Meyer, H. Müller, B. Neumann, M. Rost, K. Stupperich, G. Zech

Universität-Gesamthochschule Siegen<sup>d</sup>, D-5900 Siegen, Federal Republic of Germany

G. Alexander, G. Bella, Y. Gnat, J. Grunhaus

University of Tel-Aviv<sup>u</sup>, Israel

H. Junge<sup>v</sup>, K. Kraski<sup>w</sup>, C. Maxeiner, H. Maxeiner, H. Meyer, D. Schmidt

Universität-Gesamthochschule Wuppertal<sup>d</sup>, D-5600 Wuppertal, Federal Republic of Germany

Received 25 February 1985

<sup>a</sup> Now at Felten & Guillaume, Cologne, FRG

<sup>b</sup> Deceased

<sup>c</sup> Now at University of California at Davis, Davis, Ca., USA

<sup>d</sup> Supported by the BMFT, FRG

<sup>e</sup> Partially supported by The Norwegian Council for Science and the Humanities

<sup>f</sup> Rome University, partially supported by I.N.F.N., Sezione di Roma, Italy

<sup>g</sup> Now at CERN, Geneva, Switzerland

<sup>h</sup> Institute of Nuclear Physics, Cracow, Poland

<sup>i</sup> Now at Rutherford Appleton Laboratory, Chilton, UK

<sup>j</sup> Now at Univ. of Liverpool, Liverpool, UK

<sup>k</sup> Now at Glasgow College of Technology, Glasgow, UK

<sup>l</sup> Supported by the U.K. Science and Engineering Research Council

<sup>m</sup> Now at Texaco Europe Computer Information Systems, Hamburg, FRG

<sup>n</sup> Now at Carleton University, Ottawa, Ontario, Canada

<sup>o</sup> Now at Universität Karlsruhe, FRG

<sup>p</sup> Now at Univ. of Massachusetts, Amherst, Mass., USA

<sup>q</sup> Now at Northeastern University, Boston, Mass., USA

<sup>r</sup> Partially supported by the Department of Energy, USA

<sup>s</sup> On leave of absence from Inst. de Fisica, Universidad Federal do Rio de Janeiro, Brasil

<sup>t</sup> Now at BESSY, Berlin, FRG

<sup>u</sup> Partially supported by the Israeli Academy of Sciences and Humanities-Basic Research Foundation

<sup>v</sup> Now at Krupp Atlas Elektronik, Bremen, FRG

<sup>w</sup> Now with the firm Ernst Leitz, Wetzlar, FRG

**Abstract.** We have studied 419  $\tau$  pair events produced in the reaction  $e^+e^- \rightarrow \tau^+\tau^-$  at a c.m. energy of 34.6 GeV. We measure the cross section and angular distribution, as well as the decay branching ratios. The production characteristics are consistent with the Standard Electroweak Model predictions of  $\gamma$  and  $Z^0$  interference. The branching ratios are generally consistent with the  $\tau$  decaying according to standard weak interaction principles, but we observe somewhat more decays resulting in single charged hadrons plus neutrals than are predicted by present theory.

## Introduction

The study of pairs of  $\tau$  leptons produced in  $e^+e^-$  annihilation offers an opportunity to test many aspects of elementary particle theory. Since leptons appear to have no internal structure to complicate theoretical calculations, many definite predictions concerning the annihilation channel production of  $\tau$ 's and their subsequent decay are possible using the present understanding of weak and electromagnetic interactions.

There is still considerable experimental uncertainty about the hadronic decay properties of the  $\tau$ . This is partly due to statistical limitations; however significant systematic effects are apparent, as indicated by an almost 4 standard deviation change between the 1982 and 1984 world averages for the branching ratio into 3 charged hadrons+neutrals. Although theoretical understanding of  $\tau$ -decay to leptons and to states with an even number of hadrons seems to be on firm ground, the decays to an odd number of hadrons, which are mediated by the axial vector current, are not so well understood.

The Standard Model [1] of electroweak interactions predicts that  $e^+e^-$  annihilation to  $\tau$ -pairs can proceed by exchange of a virtual  $\gamma$  or  $Z^0$ . Equation 1 indicates the differential cross section predicted by the Standard Model, without radiative corrections.

$$s \cdot \frac{d\sigma}{d\Omega}(e^+e^- \rightarrow \tau^+\tau^-) = B(1 + \cos^2(\Theta^+)) + (8/3)A \cos(\Theta^+), \quad (1)$$

where  $A$  and  $B$  are coefficients which depend on the value of  $\Theta_w$ , the electroweak mixing angle, and  $\Theta^+$  denotes the angle between the incoming  $e^+$  and the outgoing  $\tau^+$ .

Assuming  $\sin^2(\Theta_w)=0.228$ , the contribution of the  $Z^0$  to the total cross section is only 0.3% at  $E_{c.m.}=34.6$  GeV, an effect which is below the sensitivity of our measurements. Interference between the photon and  $Z^0$ , however, is expected to produce a

measurable asymmetry in the angular distribution, as indicated by the  $\cos(\Theta^+)$  term in (1), proportional to coefficient  $A$ . The value of  $A$  is negative and increases with the center of mass energy. At  $E_{c.m.}=34.6$  GeV the expectation is  $A=-0.095$ .

Many authors [2-4] have provided predictions for the  $\tau$  decay widths and branching ratios. The widths for the leptonic decays can be calculated from basic principles of the weak interaction. Calculating the widths for hadronic decays is less straightforward. The simplest decay,  $\tau \rightarrow \nu\pi$ , can be directly related to the process  $\pi \rightarrow \nu\mu$  through lepton universality. Multi-hadron decays with an even number of pions can be related to the isovector part of  $e^+e^-$  annihilation into pions through the CVC hypothesis. The decays resulting in an odd number of pions can be less reliably estimated using PCAC and Weinberg sum rules. The  $\tau$  can also decay into strange particles. These decay widths are calculated in the same manner as the non-strange decays, but assuming Cabibbo suppression.

## Experimental Apparatus

The data analyzed here were taken with the PLUTO detector at the PETRA  $e^+e^-$  storage ring at an average c.m. energy of 34.6 GeV. The integrated luminosity was  $(42.3 \pm 0.9)$  pb $^{-1}$ , determined from large-angle Bhabha scattering events.

The detector was equipped with 13 concentric cylindrical proportional chambers in a 1.65 Tesla magnetic field. The chambers were 0.94 m long and the outermost chamber had a radius of 0.56 m. The track chambers were surrounded by lead scintillator shower counters. The barrel shower counter covered the angular region with  $|\cos(\Theta)| < 0.58$  and had a thickness of 8.6 radiation lengths. The two endcaps with  $0.58 < |\cos(\Theta)| < 0.95$  were covered by shower counters with thicknesses of 10.2 radiation lengths. Another set of lead scintillator shower counters (large angle taggers, or LAT's), which were 14.5 radiation lengths thick, covered the angular regions between 75 mrad and 260 mrad from the beam axis.

Outside the shower counters was a muon detector consisting of an iron hadron absorber and two sets of chambers at approximately 5.3 and 7.6 interaction lengths. In the angular region  $|\cos(\Theta)| < 0.6$  the inner and outer muon chambers covered respectively 67% and 90% of the solid angle. Further details of the PLUTO detector can be found in [5].

## Selection Criteria and Decay Identification

The various channels available for the decay of each  $\tau$  lead to many possible decay combinations in  $\tau$ -

pair events. Each combination has a different appearance in the detector, different types and levels of background, and a different detection efficiency.

Not all decay combinations yield useful signal to background ratios. We have therefore excluded the following configurations from our analysis:

1. both  $\tau$ 's decaying to muons
2. both  $\tau$ 's decaying to electrons
3. both  $\tau$ 's decaying to single  $\pi$ 's (or  $K$ 's)
4. both  $\tau$ 's decaying to three or more charged hadrons
5. events where one  $\tau$  decays to a  $\mu$  and the other to a single hadron.

A prominent feature of all remaining decay combinations is that at least one of the  $\tau$ 's decays to a single charged particle. At the center of mass energy used here the decay products of each  $\tau$  are usually well separated in angle, and the single charged prong will appear as an isolated track. The basic event selection strategy, which utilized visual scanning only as a check on performance, was therefore as follows:

1. Select events with at least one isolated track.
2. Assume that each such event is a  $\tau$ -pair and attempt to identify the probable decay configuration of each  $\tau$ .
3. Then apply further selection criteria, which depend on the observed decay configuration, to reduce backgrounds.

We now describe this procedure in more detail. The first step in selecting events was to reconstruct the tracks of charged particles in the tracking chambers, and analyse the energy deposited in the shower counters.

Tracks were required to have momenta in excess of 0.12 GeV/c, to be inclined to the beam line such that  $|\cos(\theta)| < 0.98$ , and to extrapolate into a cylindrical vertex region, centered at the interaction point, of radius 30 mm and extending  $\pm 200$  mm along the beam axis. Energy deposits in the shower counters of more than 0.1 GeV were either associated with the passage of charged particles or attributed to  $\gamma$ 's produced at the interaction point. Gammas which converted before reaching the shower counters ( $\sim 15\%$ ) were also identified by searching for track pairs of zero net charge whose trajectories were consistent with a conversion vertex in the wall of the beam pipe or within the tracking chambers. Because of limited resolution, no attempt was made to reconstruct  $\pi^0$ 's from the measured  $\gamma$ 's.

The next step in event selection was to require an "isolated" track as a candidate for a single-prong  $\tau$ -decay. Such an isolated track was required to be inclined to the beam line such that  $|\cos(\theta)| < 0.6$ , to

have a momentum of at least 1.0 GeV/c, to be at least  $145^\circ$  from any other track, and to have less than 0.12 GeV of shower energy in an annulus between  $35^\circ$  and  $145^\circ$  centered on the track. Extra shower energy within  $35^\circ$  of the track was allowed in order to retain decays with one charged prong accompanied by neutrals as valid single-prong candidates.

The products of each  $\tau$ -decay were then identified as  $e$ ,  $\mu$ , single hadron, single charged hadron + neutrals, hadronic multi-prong, or unidentified

**Table 1.** Decay identification criteria

1. Electron $\tau \rightarrow \nu_\tau e \nu_e$	The shower energy and momentum of an isolated track were required to be equal within errors, and each to exceed 1.0 GeV. To reject charged hadrons accompanied by $\pi^0$ 's, no more than 0.12 GeV of unassociated shower energy was allowed within a $35^\circ$ cone about the track.
2. Muon $\tau \rightarrow \nu_\tau \mu \nu_\mu$	A muon chamber hit was required within 0.5 m of the extrapolation of an isolated track. For tracks with momenta between 1.0 and 3.0 GeV/c, the inner chambers were used, while for higher momenta the outer chambers were required. The track was also required to point into the solid angle actually covered by the relevant muon chambers. No more than 1.0 GeV of shower energy could be associated with the track, and no more than 0.12 GeV of unassociated shower energy was allowed within a $35^\circ$ cone about the track.
3. Hadron $\tau \rightarrow \nu_\tau h$	A decay candidate was considered an unaccompanied $\pi$ or $K$ if it passed the same cuts as for the Muon category but failed to produce a muon chamber hit.
4. Hadron <sub>1</sub> $\tau \rightarrow \nu_\tau + 1 h^\pm + \geq 1 \pi^0$	Excess shower energy or $\gamma$ 's in the vicinity of an isolated track were considered as evidence for accompanying $\pi^0$ 's. If there was either more than 0.5 GeV of unassociated shower energy within $35^\circ$ of an isolated track, or if there was more than 1.0 GeV of associated shower energy but the track had failed to be identified as an electron because its momentum and shower energy were sufficiently different, the decay was classified as Hadron <sub>1</sub> .
5. Hadron <sub>3</sub> $\tau \rightarrow \nu_\tau + 3 h^\pm + \geq 0 \pi^0$	At least 2, and no more than 5 tracks were required in the the $35^\circ$ cone opposite an isolated track. Apparent multi-prong decays with more than 5 tracks were considered to be background, and caused rejection of the event.
6. No ID $\tau \rightarrow \nu_\tau + 1 \text{ prong}$	All one-prong decays which were not identifiable according to criteria 1-4 were nevertheless retained for further analysis. In addition, all tracks with $ \cos(\theta)  > 0.6$ were classified as No ID

single-prong according to the criteria listed in Table 1.

Backgrounds remaining in the  $\tau$ -pair candidates were then suppressed by applying requirements which in part depended on the observed decay configuration. All events were required to pass the criteria listed in Table 2. Events with less than 4 tracks were found to contain higher levels of background and were subjected to the additional criteria listed in Table 3. These included all one-prong against one-

**Table 2.** General background suppression criteria

1. *Total shower energy*: To suppress Bhabhas, the total shower energy in the barrel and endcaps was required to be less than  $1.4 \cdot E_{\text{beam}}$ .
2. *Anti-Tagging*: To suppress  $\gamma\gamma$  events no individual shower energy deposit in the LAT with more than  $0.2 \cdot E_{\text{beam}}$  was allowed.
3. *Timing*: The times at which tracks reached the barrel and endcap shower counters were used to identify and reject cosmic ray events.
4. *Residual  $e^+e^-$  background in events with Hadron<sub>3</sub>-decays*: Events with 4 or more tracks were found to be almost free of background at this point. All such events were accepted without further examination unless both the isolated track and an opposite track were identified as electrons, each with more than 30% of the beam energy.

**Table 3.** Background suppression criteria for events with less than 4 tracks

1. *Further measures against  $e^+e^-$  backgrounds*: Events were rejected if every track had over 2 GeV of associated shower energy and the total shower energy of the event exceeded  $E_{\text{beam}}$ .
2. *Special measures against  $\mu^+\mu^-$  backgrounds*: At least one isolated track was demanded which either had more than 1.0 GeV of associated shower energy or more than 0.5 GeV of un-associated shower energy within a  $35^\circ$  cone around the track.
3. *Missing Mass*: Residual Bhabhas and  $\mu$  pair events were suppressed by requiring a missing mass of more than  $E_{\text{beam}}/2$ . The missing mass squared is defined as  $\delta^2 = (2 \cdot E_{\text{beam}} - E)^2 - P^2$ , where  $E$  and  $P$  are respectively the total visible energy and momentum in the final state.
4. *Measures to suppress 2 photon processes*: The total invariant mass was required to exceed 3 GeV, and the vector sum of the transverse momenta seen in tracks was required to be at least 8% of  $E_{\text{beam}}$ , except in the case of a Muon when only 3% of  $E_{\text{beam}}$  was required.
5. *Acollinearity*: Events were rejected if any track was within  $3.3^\circ$  of being collinear with a Muon. This suppressed cosmic ray  $\mu$ 's.
6. *Acoplanarity*: All tracks were required to be more than  $3.3^\circ$  out of the plane formed by an isolated track and the beam axis. This was particularly effective against radiative Bhabhas and  $\gamma\gamma$  processes. This requirement was not made if the event contained a Muon, since in this case little background remained after the acollinearity cut was made.

prong events, and about half of all accepted hadron multi-prong decays, since often only two out of three tracks in multi-prong decays were successfully reconstructed.

After applying all criteria, a sample of 419 events was obtained. Monte Carlo simulations, described in the following section, indicate that this constitutes 23% of all  $\tau$  pair events produced with  $|\cos(\Theta^+)| < 0.6$ .

## Background Estimates and Acceptance

Cosmic ray and beam-gas backgrounds were estimated from the number of otherwise acceptable events whose vertices lay on the beam line, but far from the interaction point. Candidate background events arising from annihilation and 2 photon processes were generated in a Monte Carlo program [6, 7] and passed through a detailed simulation of the detector which included the effects of decays and interactions of the particles. The simulated events were then subjected to the  $\tau$  selection criteria. From the results a total of 28 background events are estimated to remain in the actual  $\tau$  sample. A summary is shown in Table 4.

To estimate the efficiency of the detector and analysis chain for genuine  $\tau$ -pair events, a sample of such events was generated [7] and the decay simulated using the branching ratios listed in Table 6. The resulting events were passed through the detector simulation and analysis chain. The accepted events were used to construct a four dimensional matrix,  $m_{i,j,k,l}$ , which gives the number of type  $i$  decays found in events actually of type  $k$  opposite

**Table 4.** Summary of background estimates

Type of background	Expected no. of events	Source of estimate
$e^+e^- \rightarrow e^+e^-$	$0.0 \pm 1.6$	Berends and Kleiss M.C. [7]
	< 3	visual scanning (data)
$e^+e^- \rightarrow \mu^+\mu^-$	$6.8 \pm 1.6$	Berends and Kleiss M.C. [7]
$e^+e^- \rightarrow q\bar{q}$	$5.5 \pm 2.5$	Hoyer M.C. + Feynman-Field frag. [6]
$e^+e^- \rightarrow e^+e^-e^+e^-$	$5.8 \pm 1.9$	Vermaseren M.C. [6]
$e^+e^- \rightarrow e^+e^-\mu^+\mu^-$	$0.2 \pm 0.2$	Vermaseren [6]
$e^+e^- \rightarrow e^+e^-q\bar{q}$	$0.0 \pm 2.0$	Vermaseren M.C. [6]
$e^+e^- \rightarrow e^+e^-\tau^+\tau^-$	$7.6 \pm 1.6$	Vermaseren M.C. [6]
Beam-gas + cosmic rays	$2.0 \pm 4.0$	Z sideband (data)
Total	$28 \pm 7$	

type  $l$ , but identified as type  $i$  opposite type  $j$ . A normalized matrix  $\tilde{\epsilon}_{i,j,k,l}$  was constructed from  $m_{i,j,k,l}$  by dividing each term by the total number of generated events. This matrix was utilized in the analysis described in the following sections.

To confirm the reliability of the Monte Carlo simulation, many distributions from real and simulated events were compared and good agreement was found. Some global comparisons are shown in Figs. 1-4. Figure 1 shows the momentum distribution of isolated tracks. Figure 2 shows the acollinearity distribution of all accepted events, where the acollinearity is defined as the complement of the largest angle between any two tracks in the event. Figures 3 and 4 show respectively the distributions of total event transverse momentum and missing mass.

The magnitude of systematic uncertainties in our results was estimated by varying the relevant event selection criteria and the assumptions used in the background and  $\tau$ -production Monte Carlo simulations. The principal uncertainties arise from the

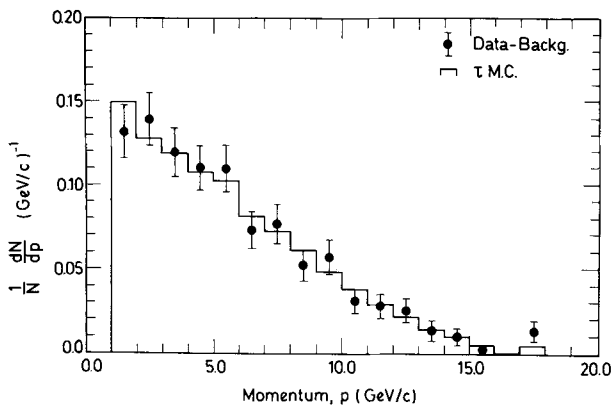


Fig. 1. Momentum distribution of all isolated tracks fulfilling the selection criteria for  $\tau$ -decays

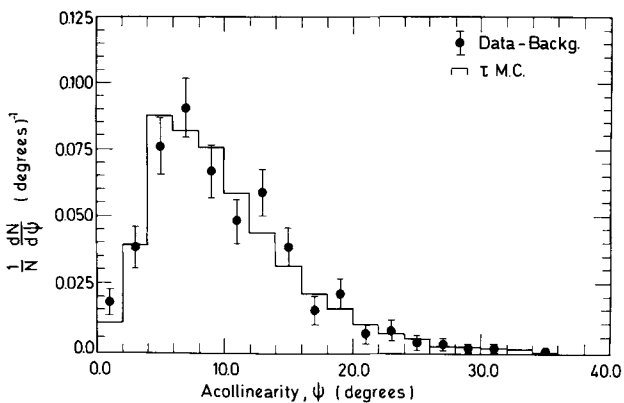


Fig. 2. Distribution of the acollinearity,  $\Psi$ , defined as the complement of the largest angle of separation between any two tracks in an event

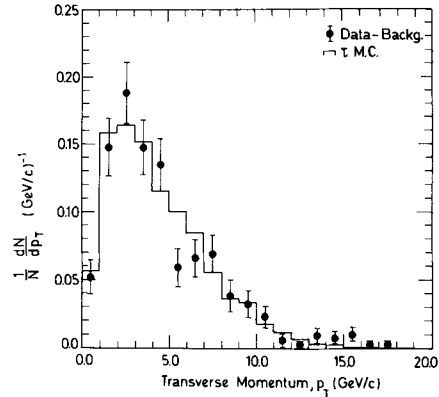


Fig. 3. Distribution of event transverse momentum, defined as the vector sum of all track momenta, projected onto the plane perpendicular to the beam axis

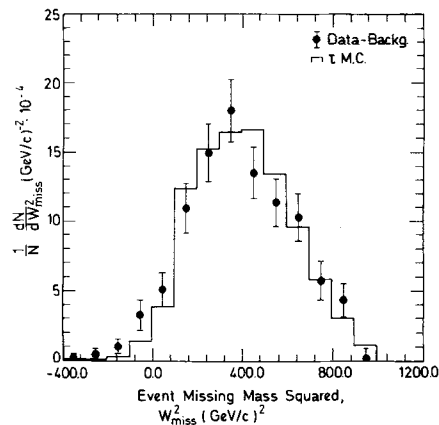


Fig. 4. Distribution of event missing mass squared,  $W_{\text{miss}}^2$ , defined as

$$W_{\text{miss}}^2 = (E_{\text{initial}} - E_{\text{visible}})^2 - (\vec{P}_{\text{initial}} - \vec{P}_{\text{visible}})^2$$

relatively poor quality of our shower detection and a lack of complete information concerning the characteristics of  $\tau$  multi-prong decays. Because we could not reconstruct  $\pi^0$ 's reliably, our ability to constrain such variations using information obtained from the data itself was limited. Appreciable uncertainty also existed in the simulation of hadronic interactions in the shower counters. Perhaps for related reasons, we found that the  $\tau$  signal varied with the threshold of the extraneous shower energy cut in a way which was not perfectly explained by the Monte Carlo. In most cases, systematic effects were found to introduce uncertainties of about 10%, but in some cases the uncertainty approached 30%.

### Branching Ratios

To decouple the branching ratio measurements from one another as much as possible, each of the  $6 \times 6$  decay category combinations was considered as a

separate process. For each combination, detection efficiencies, background levels, and crossover from other decay combinations were estimated. This information was then used in an unfolding procedure to determine the actual number of decays in each category which had occurred, regardless of whether they were accepted or correctly identified.

We adopted an unfolding technique based on direct subtraction of background and misidentified decays, rather than matrix inversion. The procedure for events which did not contain an unidentified single prong is described by (2), which yields  $N_i$ , the true number of decays of type  $i$  in terms of  $n_{i,j}$ , the number of decays of type  $i$  observed in events of type  $i$  opposite type  $j$ .

$$N_i = \eta_i \sum_{j=1}^5 (1/\tilde{E}_{i,j}) \cdot \left( n_{i,j} - b_{i,j} - \frac{1}{2} N_{\text{tot}} \cdot \sum_{\substack{k=1 \\ k \neq i}}^5 \sum_{l=1}^5 \tilde{\varepsilon}_{i,j,k,l} \right). \quad (2)$$

The branching ratios,  $\text{BR}_i$ , are then simply

$$\text{BR}_i = N_i/N_{\text{tot}}, \quad \text{where } N_{\text{tot}} = \sum_{j=1}^5 N_j. \quad (3)$$

The detection efficiency for the  $i, j$ 'th combination of decay categories where the  $i$ 'th decay is correctly identified, is denoted by  $\tilde{E}_{i,j}$ . The summation over the Monte Carlo-derived event acceptance and identification matrix  $\tilde{\varepsilon}_{i,j,k,l}$  subtracts the estimated number of decays accepted into the  $i, j$ 'th category which were incorrectly identified. The term  $b_{i,j}$  corrects for the background expected in each combination.

Some decay combinations were not accepted because of high background levels, and are therefore missing in the summation over  $j$ . The factors  $\eta_i$  compensate for these excluded combinations.  $N_{\text{tot}}$ , the total number of decays, and the  $\eta_i$  were calculated using the measured branching ratios in a rapidly converging iterative procedure. The results were

**Table 6.** Branching ratio results for  $\tau \rightarrow \nu_\tau X$

	$e \nu_e$	$\mu \nu_\mu$	$1 h^\pm$ $0 \pi^0$	$1 h^\pm$ $\geq 1 \pi^0$	$3 h^\pm$ $\geq 0 \pi^0$
Without No ID events	0.131 $\pm 0.020$	0.192 $\pm 0.016$	0.131 $\pm 0.021$	0.433 $\pm 0.021$	0.120 $\pm 0.013$
Only No ID events	0.116 $\pm 0.071$	0.279 $\pm 0.12$	0.072 $\pm 0.12$	0.315 $\pm 0.086$	0.194 $\pm 0.079$
Weighted average (stat.) (syst.)	0.130 $\pm 0.019$ $\pm 0.029$	0.194 $\pm 0.016$ $\pm 0.017$	0.130 $\pm 0.020$ $\pm 0.040$	0.427 $\pm 0.020$ $\pm 0.029$	0.122 $\pm 0.013$ $\pm 0.039$
Theoretical prediction (see text)	0.175 $\pm 0.007$	0.170 $\pm 0.007$	0.114 $\pm 0.004$	0.245 $\pm 0.010$	0.051 $\pm 0.002$
1984 World average [8]	0.165 $\pm 0.009$	0.185 $\pm 0.011$	0.103 $\pm 0.012$	0.378 $\pm 0.023$	0.170 $\pm 0.013$
Monte Carlo values (input)	0.170	0.179	0.082	0.429	0.141

found to be independent of the initial values assumed for the branching ratios.

Separate results were similarly obtained for the 56 events containing unidentified single prong decays, and these were averaged with the results from the rest of the sample.

It should be noted that the resulting branching ratios are independent of assumptions about the total  $e^+ e^- \rightarrow \tau^+ \tau^-$  cross section. The estimated background and crossover in each decay category are shown in Table 5, together with the observed number of decays. The branching ratio results are shown in Table 6.

The 1984 World Average [8] gives an upper limit of 1.4% for the branching ratio of  $\tau \rightarrow 5(\pi^\pm) \nu_\tau$ . Aihara et al. [9] give a limit of 0.3%. Such decays were not included in the Monte Carlo simulation, nor were other decays of the type:  $\tau \rightarrow 5(\pi) \nu_\tau$ . There was one decay in the sample compatible with a final state of either 5 charged  $\pi$ 's or 3 charged  $\pi$ 's together with  $\gamma$ 's that converted in the beam pipe or in the first few inner track detector chambers. Owing to

**Table 5.** Sample, background, and crossover in each decay category

	Electron	Muon	Hadron	Hadron <sub>1</sub>	Hadron <sub>3</sub>	No ID
Sample	105	170	56	308	143	56
Background	-9	-13	-1	-16	-10	7
Crossover	-26	-4	-10	-37	-18	-
Data after background and crossover subtraction	70	153	45	255	115	49

The numbers presented in each column are sums over the 6 possible decay configurations for the opposite decay in the event. When calculating the branching ratios and  $\sigma_{\text{total}}$ , each combination was used separately

the difficulty of reliably determining the detection efficiency for 5-prong decays and separating them from 3-prongs with pair conversions, the branching ratio for all final states with 3 or more charged hadrons is given, and no limit is placed on the rate of 5-prong production.

We observe no significant discrepancy between our results and the present world averages. In particular, our values for the topological branching ratios to one and three prongs, ( $B_1 = 0.878 \pm 0.013 \pm 0.039$ ), and ( $B_3 = 0.122 \pm 0.013 \pm 0.039$ ), are in agreement with recent measurements [9]. Our results are also in general accord with theoretical predictions [2]. The theoretical branching ratios shown in Table 6 are those of Gilman and Rhie [3], rescaled to correspond to a total  $\tau$ -lifetime of  $2.79 \cdot 10^{-13}$  s. This scaling ensures that the leptonic branching ratio ( $e + \mu$ ) corresponds to the world average value [8]. Only the reliably calculable decay channels  $e\nu$ ,  $\mu\nu$ ,  $\pi$ ,  $K$ ,  $\pi\pi$ ,  $\pi K$ ,  $4\pi$ , and  $6\pi$  are included, and are seen to contribute  $(75 \pm 3)\%$  of all  $\tau$ -decays. The axial-vector current, coupling to states with an odd number of hadrons, can account within large uncertainties for the remaining 25% of all decays [2, 4]. It has, however, been pointed out that these neglected axial vector decays should result in more multi-prong than single-prong states on the basis of isotopic spin arguments [3]. From the difference between the measured and theoretical branching ratios in the last two columns of Table 6, our data indicate that the modes excluded from the calculation contribute  $(18.2 \pm 3.5)\%$  of the total  $\tau$  branching fraction as single-prong decays accompanying neutrals, but only  $(7.1 \pm 4.1)\%$  as multi-prong decays. According to these results, the probability that multi-prongs actually constitute more than half of these decays is only 2%, although we point out that the systematic component of our errors is large. Our results then lend weak support to the conclusion of [3] that discrepancies exist in our understanding of  $\tau$ -decay.

### Production Cross Section and Asymmetry

We determined the total cross section for  $\tau$ -pair production by comparing the total number of decays,  $N_{\text{tot}}$ , which resulted from the branching fraction analysis, with a corresponding number derived from the complete Monte-Carlo simulation of  $\tau$ -production according to the Standard Model, incorporating weak interference and radiative corrections to order  $\alpha^3$  [7]. We express our result as the ratio of the observed and the predicted cross sections

$$\frac{\sigma_{\text{total}}(\text{measured})}{\sigma_{\text{total}}(\text{expected})} = 0.89 \pm 0.05 (\text{stat.}) \pm 0.08 (\text{syst.}).$$

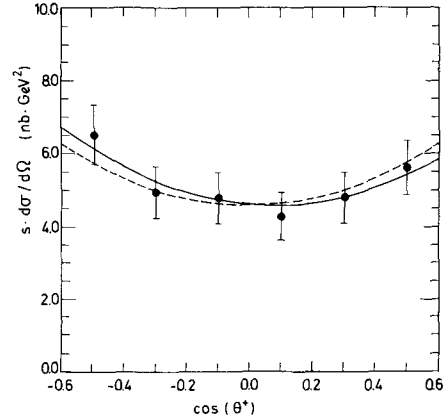


**Fig. 5.** Invariant differential  $\tau$  production cross section,  $s \cdot d\sigma/d\Omega$ , corrected for radiative effects. The solid line is a fit to (1) with  $A$  and  $B$  as free parameters. The dashed line is a fit with  $A=0$ , corresponding to the angular dependence of the pure QED expectation. The error bars do not include an overall normalization error of  $\pm 9.4\%$ .

The cross section for  $\tau$ -production is thus seen to be consistent with the Standard Model.

We then determined the invariant differential cross section,  $d\sigma/d\Omega$ , by correcting the raw  $\cos(\theta^+)$  distribution for background, radiative effects and detector efficiency, and normalizing the result to agree with our measurement of the total cross section. A fit to (1) with  $A$  and  $B$  as free parameters yielded

$$A = -0.059 \pm 0.068 (\text{stat.})_{-0.025}^{+0.0} (\text{syst.}),$$

with a  $\chi^2$  of 0.97 for four degrees of freedom. The invariant differential cross section and the result of the fit are shown in Fig. 5. The negative systematic error on the asymmetry is due to the possible presence of Bhabha events with their inherent asymmetry of almost +1.0. Although Monte-Carlo studies indicate that there should be no background from this source, its importance led us to scan the sample visually for conceivable Bhabha candidates. Only three were found. Systematic errors due to a possible helical deformation of the inner detector have been found to be negligible [11]. Our measured asymmetry is in agreement with the predictions of the Standard Theory, but is also consistent with zero. If the effects of the  $Z^0$  are suppressed by setting  $A$  to zero, the fit remains good with a  $\chi^2$  of 1.4 for 5 degrees of freedom.

### Conclusions

In conclusion, we have measured values for the branching ratios, total cross-section, and angular asymmetry in the production and decay of  $\tau$ -leptons produced in  $e^+ e^-$  annihilation at a c.m. energy of

34.6 GeV. These values are in agreement with present world averages and generally confirm theoretical expectations based on the Standard Model of electroweak interactions and the interpretation of the  $\tau$  as a sequential heavy lepton. Our results for the topological branching ratios of hadronic  $\tau$ -decays support recent measurements [9], and show that the  $\tau$  decays somewhat more frequently to a single charged particle + neutrals than can be explained according to present theoretical understanding.

*Acknowledgements.* We are indebted to the PETRA machine group and the DESY computer center for the excellent service provided during the experiment. We gratefully acknowledge the efforts of all the engineers and technicians from the various participating institutions who took part in the construction and maintenance of the apparatus. The visiting groups wish to thank the DESY directorate for the support and hospitality extended to them.

## References

1. A. Salam: Rev. Mod. Phys. **52**, 525 (1980); S.L. Glashow: Rev. Mod. Phys. **52**, 539 (1980); S. Weinberg: Rev. Mod. Phys. **52**, 515 (1980); S. Weinberg: Phys. Rev. Lett. **12**, 1264 (1967); A. Salam: Proceedings of the 8<sup>th</sup> Nobel Symposium (1968); S.L. Glashow: Nucl. Phys. **22**, 579 (1961)
2. H.B. Thacker, J. Sakurai: Phys. Lett. **36B**, 103 (1971); Y.S. Tsai: Phys. Rev. **D4**, 2821 (1971); N. Kawamoto, A.I. Sando: Phys. Lett. **76B**, 446 (1978); F.J. Gilman, D.H. Miller: Phys. Rev. **D17**, 1846 (1978); D.A. Geffen, W.J. Wilson: Phys. Rev. **D18**, 2488 (1978); T.N. Pham, C. Roiesnel, T.N. Truong: Phys. Lett. **78B**, 623 (1978); H. Goldberg, R. Aaron: Phys. Rev. Lett. **42**, 339 (1979)
3. F.J. Gilman, S.H. Rhic: SLAC-PUB-3444, Sept. 1984 (unpublished)
4. Tran N. Truong: Phys. Rev. **D30**, 1509 (1984)
5. L. Criegee, G. Knies: Phys. Rep. **83**, 152 (1982)
6. P. Hoyer et al.: Nucl. Physics **B161**, 349 (1979); R.D. Field, R.P. Feynman: Nucl. Phys. **B136**, 1 (1978); J.A.M. Vermaseren: Proceedings of the International Workshop on  $\gamma\gamma$  Interactions, Amiens (1980). Lecture Notes in Physics 134. Berlin, Heidelberg, New York: Springer 1980
7. F.A. Berends, R. Kleiss: Nuclear Phys. **B177**, 237 (1981); F.A. Berends, R. Kleiss, S. Jadach: Nucl. Phys. **B202**, 63 (1982)
8. Particle Data Group: Rev. Mod. Phys. **56**, No.2, Part II (1984)
9. C.A. Blocker et al. (MARK II): Phys. Rev. Lett. **49**, 1369 (1982); H.J. Behrend et al. (CELLO): Phys. Lett. **114B**, 282 (1982); H.J. Behrend et al. (CELLO): Z. Phys. C – Particles and Fields **23**, 103 (1984); H. Aihara et al. (TPC): Phys. Rev. **D30**, 2436 (1984); M. Althoff et al. (TASSO): Z. Phys. C – Particles and Fields **26**, 521 (1985)
10. W. Ruckstuhl: Talk at the Topical Conference of the 1984 SLAC Summer Institute on Particle Physics, July 23–Aug. 3, 1984 (unpublished)
11. Ch. Berger et al. (PLUTO): Z. Phys. C – Particles and Fields **21**, 53 (1983)